

Influence of gas pressure on the effective thermal conductivity of ceramic breeder pebble beds



Weijing Dai^a, Simone Pupeschi^b, Dorian Hanaor^{a,c}, Yixiang Gan^{a,*}

^a School of Civil Engineering, The University of Sydney, Sydney, Australia

^b Institute for Applied Materials, Karlsruhe Institute of Technology (KIT), Germany

^c Institute for Materials Science and Technologies, Technical University of Berlin, Germany

HIGHLIGHTS

- This study explicitly demonstrates the influence of the gas pressure on the effective thermal conductivity of pebble beds.
- The gas pressure influence is shown to correlate to the pebble size.
- The effective thermal conductivity is linked to thermal-mechanical properties of pebbles and packing structure.

ARTICLE INFO

Article history:

Received 4 October 2016

Received in revised form 17 February 2017

Accepted 14 March 2017

Keywords:

Effective thermal conductivity

Ceramic breeding materials

Pebble beds

Granular materials

Gas pressure

ABSTRACT

Lithium ceramics have been considered as tritium breeder materials in many proposed designs of fusion breeding blankets. Heat generated in breeder pebble beds due to nuclear breeding reaction must be removed by means of actively cooled plates while generated tritium is recovered by purge gas slowly flowing through beds. Therefore, the effective thermal conductivity of pebble beds that is one of the governing parameters determining heat transport phenomenon needs to be addressed with respect to mechanical status of beds and purge gas pressure. In this study, a numerical framework combining finite element simulation and a semi-empirical correlation of gas gap conduction is proposed to predict the effective thermal conductivity. The purge gas pressure is found to vary the effective thermal conductivity, in particular with the presence of various sized gaps in pebble beds. Random packing of pebble beds is taken into account by an approximated correlation considering the packing factor and coordination number of pebble beds. The model prediction is compared with experimental observation from different sources showing a quantitative agreement with the measurement.

© 2017 Elsevier B.V. All rights reserved.

1. Introduction

The lithium orthosilicate, Li_4SiO_4 , is one of the most widely investigated lithium ceramic materials in the design of the tritium breeding blanket [1–9]. To maintain the tritium breeding efficiency and reduce the occurrences of mechanical failure including crushing, creeping and swelling, the material form is chosen to be pebble beds instead of directly using sintering blocks [10]. The lithium breeder beds consist of solid phase (nearly spherical-shaped solid particles) and a gas phase (helium) that fills the voids between pebbles. Although the pebble bed has better mechanical stability than sintering blocks, the effective thermal conductivity of the pebble beds is considerably lower than the intrinsic thermal conductivity

of Li_4SiO_4 due to the discrete nature of the structure and the existence of the gaseous phase of low thermal conductivity. Therefore, an adequate blanket design is crucial to remove the heat generated inside the pebble bed to guarantee the optimal bed performance for the tritium breeding and extraction. For the design of the cooling system, the effective thermal conductivity of the pebble bed is of primary importance. Many studies have investigated this property experimentally and theoretically [1–3,11]. In general, the effective thermal conductivity of the Li_4SiO_4 pebble beds in different measurement conditions falls into the range around 0.75–1.2 W/mK that is about 4 times lower than thermal conductivity of bulk Li_4SiO_4 . Not only the intrinsic properties of the constituent phases of the pebble beds but also other parameter such as the gas pressure, the pebble size, the packing structure, the external loading and other controllable parameters can affect the effective thermal conductivity [1,12].

* Corresponding author.

E-mail address: yixiang.gan@sydney.edu.au (Y. Gan).

For the Li_4SiO_4 pebble beds, the thermal conductivity ratio between the solid and the gas phase is small. As a result, it is found experimentally that the increase of the contact area introduced by the external loading contributed little to the thermal transport [6,12,13]. While varying the gas pressure is proved to alter the effective thermal conductivity of the pebble beds because the vacancies in the pebble beds are small enough to trigger the Smoluchowski effect in the gas phase [1]. However, only has a few theoretical models considered this gas pressure dependency behaviour [14–17], and such models did not consider explicitly the gas gap conduction at the scale of individual pebbles. To contribute the complete picture between experimental observation and the theoretical explanation, a numerical framework is put forward in this work to illustrate the gas pressure dependency of the effective thermal conductivity of the Li_4SiO_4 pebble beds. Recent work measured a gas pressure drop inside the pebble bed [5], which implies an influence of a non-uniform gas pressure distribution inside the beds on the overall bed performance. During operation cycles, the actual gas pressure inside the bed may differ from the designed value, resulting in a non-uniform distribution of effective thermal conductivity. Such inhomogeneous distribution may cause local heat accumulation inside pebble beds. Design and operation of tritium breeding pebble beds should consider the variation of gas pressure.

This numerical framework is designed to simulate thermal transport processes in the assemblies of individual contact units and then predict the overall thermal conductivity of pebble beds consisting of poly-disperse particles. The relation between the gas pressure effect and particle size is explored. The model prediction shows a quantitative agreement with experimental measurements of the ceramic pebble beds, in particular the gas pressure dependent behaviour.

2. Numerical framework

This numerical framework mainly consists of two parts, the finite element simulation of a representative unit and the homogenisation to assemble the units to predict the effective thermal conductivity. Since this framework is mainly focus on investigating the relation between the gas pressure and the effective thermal conductivity, a model to describe the behaviour of gas heat transfer regarding to the change of gas pressure is prerequisite.

2.1. Gas heat transfer model

In the breeder pebble beds, gases can be recognised as stagnant bulk materials because the purge speed of gases inside the beds is small enough to consider the gases as static. In practise, the thermal conductivity of a gas having a viscosity of μ can be predicted by the modified Eucken equation as

$$k_{\text{Eu}} = \frac{9\gamma - 5}{4} * \frac{C_V}{\mu} \quad (1)$$

where $\gamma = \frac{C_p}{C_V}$, is the adiabatic gas constant. C_p and C_V are specific heat at constant gas pressure and constant volume respectively [18].

However, Eq. (1) is applicable when the characteristic length of the space occupied by the gas is much larger than the mean free path of the gas molecules. When the mean free path of the gas molecules is comparable to the characteristic length of the space, the gas thermal conductivity is reduced and the Eucken equation is no longer valid. This phenomenon is called Smoluchowski effect. To quantitatively describe the Smoluchowski effect, the mean free path of the gas molecules needs to be calculated first. As the viscous

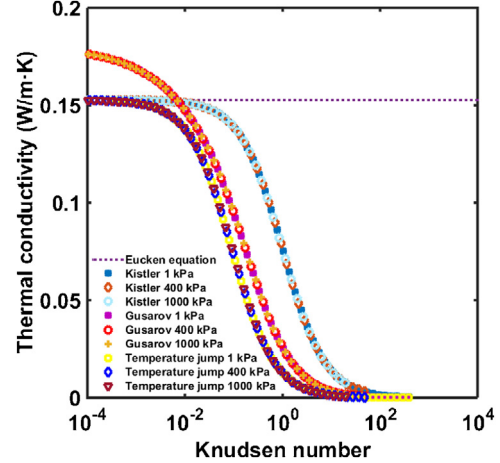


Fig. 1. Helium thermal conductivity predicted by the Gusalov's model, the temperature jump model and the Kistler's model.

ity of gases is able to be measured in labs and given by an empirical function as [19]

$$\mu_{\text{He}} = 1.865 * 10^{-5} * \left(\frac{T}{273.16} \right)^{0.7} \quad (2)$$

and according to the kinetic theory, the mean free path l can be calculated by

$$l = \frac{\mu}{P} \sqrt{\frac{\pi R T}{2M}} \quad (3)$$

where P is the pressure of the gas, T is the temperature of the gas, M is the molar mass of the gas and R is the gas constant. The Knudsen number $\text{Kn} = l/d$, defined as the mean free path l of the gas molecules over the characteristic length d of the space filled by the gas, is introduced to evaluate the significance of the Smoluchowski effect. A model derived by A.V. Gusalov [18] based on a two parallel plates geometry is applied to explain the dependency of heat transfer coefficient h upon the Kn . When the d is approaching zero (i.e., $\text{Kn} \gg 100$), the heat transfer coefficient is reaching the free molecular limit h_0 , defined as

$$h_0 = \frac{1}{4} \frac{\gamma + 1}{\gamma - 1} P \left(\frac{2R}{\pi M T} \right)^{\frac{1}{2}} \quad (4)$$

When Kn decreases, the h follows

$$h = \frac{h_0}{2} \left(\frac{1}{1 + 1/(\chi * \text{Kn})} + \frac{1}{\left(1 + \sqrt{1/\chi * \text{Kn}} \right)^2} \right) \quad (5)$$

in which $\chi = \frac{2\sqrt{\pi}}{3} \frac{9\gamma - 5}{\gamma + 1}$.

The thermal conductivity of helium of 293 K at different gas pressure predicted by different models are compared in Fig. 1, including the temperature jump model and the Kistler model [20]. The Kistler model has the simplest form, $k_K = \frac{k_{\text{Eu}}}{1+\text{Kn}}$. The temperature jump model adopts a similar form, $k_{\text{TJ}} = \frac{k_{\text{Eu}}}{1+j/d}$ in which jump distance j is proportional to mean free path l and depends on gas type. Although the Knudsen number Kn is missing in the equation, j/d can be considered to be proportional to Kn . The apparent thermal conductivity ($k_{\text{apparent}} = h * d$) that is converted from the heat conductance coefficient directly obtained from the Gusalov model is used in the plot. All the models show the S shape of the helium thermal conductivity when the Knudsen number is varying. It can be seen from Fig. 1 that the Knudsen number is the essential parameter determining the thermal conductivity of gases, combining the

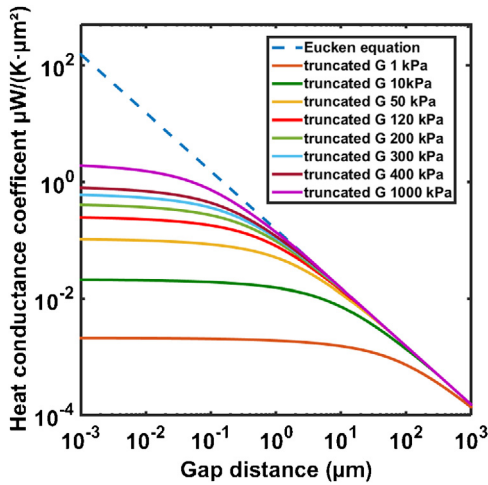


Fig. 2. Heat conductance coefficient of helium by the truncated Gusharov model (truncated G.) at 293 K with Helium pressure varying.

effects of the characteristics of gases and the geometry of spaces. However, the Gusharov model over predict the thermal conductivity when the Knudsen number drops beyond 0.01. Thus, the part above the horizontal line drawn by the Eucken equation is truncated. Afterwards, the helium heat conductance coefficient applied in this study is presented in Fig. 2.

2.2. Finite element simulation

The finite element simulation of a contact unit model is performed to obtain the representative thermal conductivity k_{cont} of one representative contact unit using the commercial finite element analysis (FEA) software (ABAQUS, [21]). In the FEA, the contact unit consists of two identical hemispheres contacting each other at a centre point. A constant temperature difference ΔT between two surfaces is maintained through the simulation, which results in a constant heat flux ϕ through the upper surface and lower surface at the surfaces at steady states, conceptually presented in the Fig. 3. Thus, the representative thermal conductivity of the contact unit is to be calculated by the Fourier's law, $k_{\text{cont}} = \frac{\phi D}{\Delta T A}$, in which D and A are the diameter and the cross-sectional area of the hemisphere.

In reality, a gaseous phase present in the void space between two hemispheres transfers the heat between two spherical surfaces. However, the thermal conductivity of the gaseous phase is not uniform in this model, which is complicated to implement. To maintain the simplicity of the numerical simulation but preserve the accuracy of the definition, we apply a distance-dependent thermal gap conductance (*GAP CONDUCTANCE in the ABAQUS software) between two spherical surfaces instead of creating additional phases, e.g., no additional dedicated elements for the gas phase. The magnitude of the thermal gap conductance follows the modified Gusharov's model introduced in the previous section, shown in Fig. 2.

2.3. Effective thermal conductivity

To derive the effective thermal conductivity k_{eff} of pebble beds from the properties of contact units, the topological characteristics of pebble beds must be considered, i.e., the contact network of packed pebbles. Although by implementing discrete element methods (DEM) the detailed geometry can be simulated [22–24], those methods require significant computational efforts. Therefore, a concise approximation is preferred in this study. Batchelor and O'Brien [25,26] derived a model to predict the effective thermal conductivity of granular materials comprising identical spheres

having a radius of r and a solid thermal conductivity of k_s . In this prediction, a similar contact unit is established to calculate heat flux φ transferring through the contact unit exhibiting a temperature difference of ΔT . A non-dimensional heat flux $\mathcal{H} = \frac{\phi}{\pi r k_s \Delta T}$ is used for simplification. The effective thermal conductivity is attributed by the network of the contact units throughout the entire granular material. An integration of heat flux over surface of all spheres which representing the contact network gives the total heat flux across the entire volume of the granular material. Based on this theorem, the estimation equation [26] based on the volume fraction f and coordination number N_c is drawn as

$$\frac{k_{\text{eff}}}{k_s} = \frac{1}{2} f N_c \mathcal{H} \quad (6)$$

A similar equation was derived by Gusharov and Kovalev [14] for a randomly packed structure of mono-sized spheres. In practice, pebbles are nearly spherical in shape, which makes it possible to apply the above equation. Although pebbles vary in size, a bed of mono-sized pebbles of a reasonable average size is supposed to be representative. To use this prediction, the heat flux ϕ computed from the finite element simulation described in the previous section is used. As the non-dimensional heat flux \mathcal{H} is calculated, the effective thermal conductivity is evaluated with knowing volume fraction f and coordination number N_c . Experimentally, volume fraction can be obtained easily but coordination number requires sophisticated test equipment and data processing [24,27].

2.4. Estimation of coordination number

Following the above discussion, this section introduces a correlation between volume fraction f and coordination number N_c . Experimentally, the detail information of coordination number can be measured by X-ray detection with image analysis techniques. However, it is not efficient to measure every pebble bed and the scale of beds being measured is limited by the detection machine. Therefore, a proper estimation of the average coordination number of the pebble beds is necessary to predict the effective properties. A theoretical estimation of sphere beds was proposed by the Suzuki and Oshima [28,29] later validated by G.A. Georgalli and M.A. Reuter [30]. This theoretical estimation can take the particle size distribution and volume fraction of the pebble beds into account, which is relevant to the fusion blanket application. In Suzuki and Oshima's model, there is only one adjustable model parameter α

$$\alpha = \frac{2 - \sqrt{3}}{4} * \bar{N}_{ci} \quad (7)$$

where \bar{N}_{ci} is the coordination number of a sphere bed having the same volume fraction f but consisted of uniformly sized spheres. Varying volume fraction change the corresponding coordination number as well as the α according to Eq. (7). The correlation between f and \bar{N}_{ci} of regular packing structure, including simple cubic, body-centred cubic, face-centred cubic and hexagonal closed packing, can be used to calculate α . By selecting the \bar{N}_{ci} of the regular packing with similar volume fraction f to the investigated granular materials, the corresponding α is acquired and used to estimate the coordination number, and more details should be referred to the literature mentioned above.

3. Result and discussion

To validate our theoretical framework, the current European reference breeding material (properties listed in Table 1), i.e., Li₄SiO₄ pebbles, fabricated by melting-spraying [31] is used as the object in

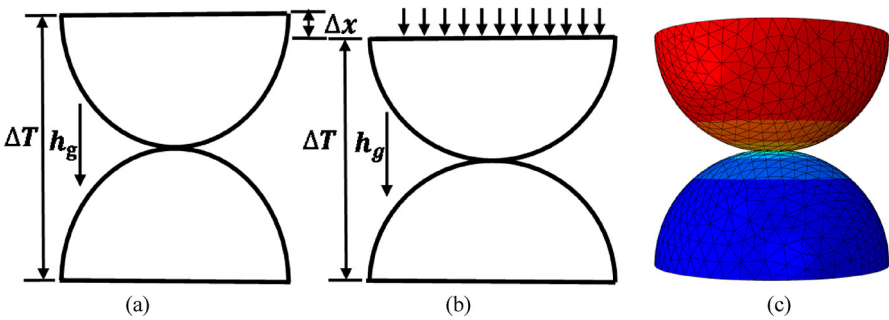


Fig. 3. Schematic drawing of contact unit model: (a) two hemispheres in contact without mechanical loading; (b) The contact under a constant mechanical loading; (c) The FEM model with temperature profile with an arbitrary unit. Here, ΔT , Δx , h_g denote the temperature difference, particle deformation, and heat flux through the gas phase, respectively.

Table 1
Li₄SiO₄ properties (T = 293 K) [32,33].

Thermal conductivity k_s	4.881 $\mu\text{W}/\mu\text{m}^*\text{K}$
Specific heat C_p	$8.99 \times 10^8 \mu\text{J}/\text{kg}^*\text{K}$
Density ρ	$2.28 \times 10^{-15} \text{ kg}/\mu\text{m}^3$
Young's modulo	$8.849 \times 10^{-2} \text{ N}/\mu\text{m}^2$
Poisson ratio	0.24

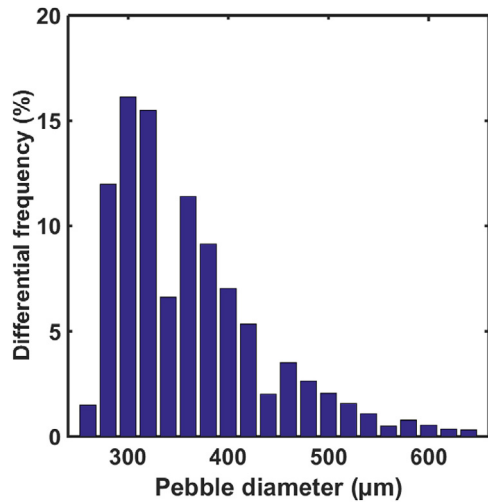


Fig. 4. Size distribution of the pebbles.

this study. Particle size distribution is shown in Fig. 4 with size ranging from 250 μm to 650 μm and an average particle size is about 350 μm . The effective thermal conductivity of this pebble bed is measured by the hot wire method in helium gas environment with variable gas pressure.

3.1. Mechanical load

First, influence of external mechanical loading on effective thermal conductivity of pebble beds is examined in order to validate the assumption of the point-contact mode in the following studies. In the simulation, the contact unit is compressed by a series of predefined length but maintaining the constant temperature difference between the top and the bottom surfaces. For each compression case, the compression force and total heat flux on the top surface of the contact unit is calculated. Gan and Kamlah [34] proposed a model to approximate the apparent mechanical loading on a pebble bed based on the average contact force. We treat the simulated compression force as the average contact force and use the model to calculate external mechanical loading, more details can be found in [34]. After that, a relation of the representative ther-

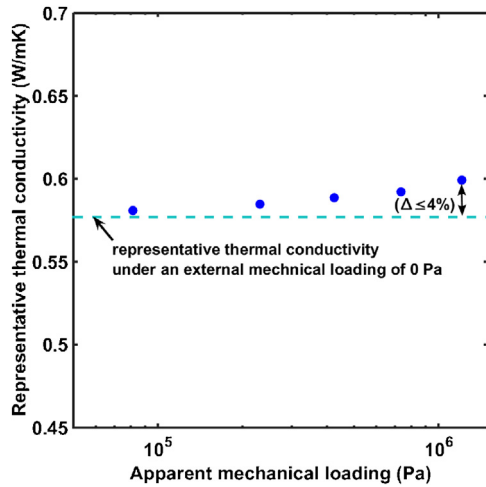


Fig. 5. Influence of external mechanical loading on the contact unit of $D = 350 \mu\text{m}$, and the helium gas pressure is 120 kPa.

mal conductivity of contact units versus the external mechanical loading on a pebble bed is plotted in Fig. 5. The Fig. 5 presents variance of the representative thermal conductivity of the contact unit, $D = 350 \mu\text{m}$, when the external mechanical loading ranging from 0.08 MPa up to 1.2 MPa. The representative thermal conductivity of the contact unit only increases slightly ($\leq 4\%$), when the external mechanical loading exceeds 1 MPa. This numerical result shows consistency with the experimental observations in the literature [6,12,13] that external mechanical loading playing a minor role in varying the effective thermal conductivity of the pebble beds when external mechanical loading does not exceed 1 MPa. Therefore, it is reasonable to concentrate on the influence of the gas pressure in the pebble beds and neglects the external mechanical loading, i.e., only point contact cases were studied in the rest of the result section.

3.2. Size dependency

The representative thermal conductivity of contact units of different sizes were first examined according to the result of the finite element simulation, shown in Fig. 6. Contact units of four sizes (sphere diameter $D = 250 \mu\text{m}$, $350 \mu\text{m}$, $500 \mu\text{m}$, and $650 \mu\text{m}$) were simulated in the Abaqus software. The representative thermal conductivities of these four contact units have a similar positive relation with gas pressure, increasing as gas pressure rises up. This result consists with the observation of the effective thermal conductivity of pebble beds under various magnitudes of helium pressure [1]. Such a trend of the representative thermal conductivity is consistent with the upward shift of the heat conductance

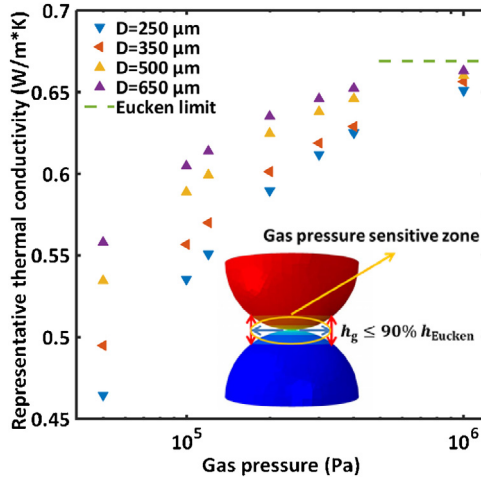


Fig. 6. Gas pressure related size dependency of the contact units.

coefficient of helium when gas pressure increases shown in Fig. 2. Additionally, a size dependency is shown by the simulation with a smaller contact unit bringing about a decrease in representative thermal conductivity. Such size dependency is significant when the gas pressure is low. A gas pressure sensitive region is defined to explain this gas pressure related size dependency. As shown in the insert of Fig. 6, the gas pressure sensitive region is restricted by a boundary at which heat conductance coefficient of helium is equal to 90% of the magnitude calculated by the Eucken equation at the same gas pressure. Even though the area of the gas pressure sensitive zone is relative small, the effect of gas pressure is still obvious in these contact units. When helium pressure is as low as 50 kPa, a cross-sectional area ratio of a corresponding sensitive zone to a total cross-section of the contact unit is 15% and 6% for $D = 250 \mu\text{m}$ and $D = 650 \mu\text{m}$, respectively. This contrast indicates that for a contact unit of a smaller diameter, a larger portion of the surface of the hemisphere is influenced by the Smoluschowski effect. Since the Smoluschowski effect deteriorates heat transfer ability of helium, the overall ability of contact units to transfer heat is weakened. While the helium pressure is elevated up to 1000 kPa, such cross-sectional area ratio becomes 2% and 1% for $D = 250 \mu\text{m}$ and $D = 650 \mu\text{m}$, respectively, which means almost all surface of both contact units escapes from the Smoluschowski effect. It can be seen from Fig. 6, the representative thermal conductivity of the four contact units start to converge towards the Eucken limit that is acquired by neglecting the Smoluschowski effect and applying heat conductance coefficient of the dashed line in Fig. 2 in the finite element simulation. Thus, due to diminution of the gas pressure sensitive zone along with elevation of the gas pressure, deterioration of the representative thermal conductivity of contact units vanishes.

3.3. Effective thermal conductivity of the pebble bed

According to the methodology introduced in the previous sections, volume fraction f and coordination number N_c is required to estimate the effective thermal conductivity. The volume fraction of the pebble bed was experimentally measured as about 0.64 and close to the volume fraction of a BCC packing of 0.68, so the coordination number of the BCC packing of 8 was used as the \bar{N}_{ci} to adjust α properly in Eq. (7) in the calculation of the average coordination number based on the Suzuki and Oshima's model [28,29]. The model was further fed with the size distribution shown in Fig. 4, and the resultant average coordination number was 7.8 for this poly-dispersed pebble bed. A mono-size pebble bed of the

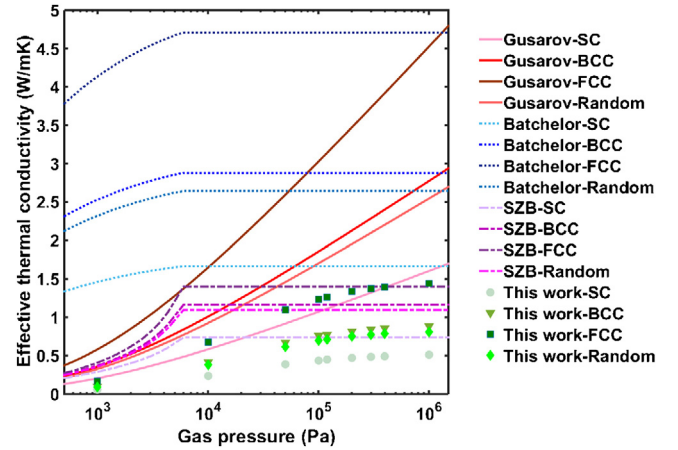


Fig. 7. Effective thermal conductivity predicted by the Gusarov's model, the SZB model, the modified Batchelor's model, and the proposed framework.

same volume fraction and coordination number with size of pebbles equal to the average size $350 \mu\text{m}$ is assumed to represent this poly-disperse one. This assumption may introduce potential uncertainty but should be acceptable in an average sense. Recalling Eq. (6), after nondimensionalisation of heat flux of the contact unit of $D = 350 \mu\text{m}$ computed by simulation, the effective thermal conductivity of the pebble bed can be obtained by rearranging Eq. (6) as $k_{\text{eff}} = \frac{1}{2}fN_c\mathcal{H}k_s$. Besides, the effective thermal conductivity of SC, BCC and FCC packing were calculated through the same procedure. In addition, the original model developed by Batchelor, the model proposed by Gusarov and the Schlunder-Zehner-Bauer (SZB) model were supplied with the identical parameter and the gas heat conductance coefficient discussed before. The results were compared with the current work as shown in Fig. 7.

The original Batchelor's model omitted the Smoluschowski effect in gas phase and consequently the effective thermal conductivity given by the model was independent of gas pressure. However in order to examine the effect of gas pressure, a slight modification inspired by the Gusarov's model [18] is adopted. In this modification, the length of contact units is considered as the characteristic length to compare with the mean free path of gas at given gas pressure to obtain the Knudsen number. The gas pressure dependency of the effective thermal conductivity of this numerical framework and the Gusarov's model expands over the entire span of investigated gas pressure. However, when helium pressure approaches 1000 kPa, the effective thermal conductivity predicted by this framework converges towards an upper bound and such an upper bound can be concluded with the Eucken limit discussed in the analysis of individual contact unit. For the modified Batchelor's model and the SZB model, a saturation phenomenon of the effective thermal conductivity appears at helium pressure of about 10 kPa and afterward saturated conductivity is maintained in the rest range of helium pressure. It is because in this range, the Knudsen number is small enough to overlook the Smoluschowski effect and the helium thermal conductivity is constant. The sharp transition in the SZB model is caused by the truncation of heat conductance coefficient above the Eucken limit mentioned in the previous section. In contrast, the effective thermal conductivity of the Gusarov's model exhibits an infinite monotonic function depending on increase of helium pressure increases within the investigated range. One of the reasons to explain this indefinite increase of the effective thermal conductivity of the Gusarov's model is overestimate of gas thermal conductivity discussed in the previous section. Although similar formulas have been used to estimate gas heat conductance coefficient, a cut-off mechanism was imposed in other models to avoid

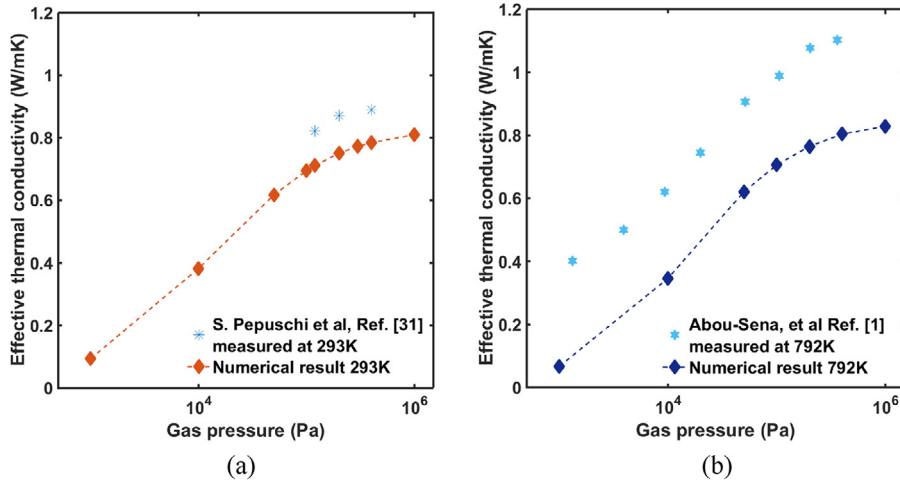


Fig. 8. Effective thermal conductivity comparison between model predictions and experiments data from: (a) S. Pepuschi et al. [31] and (b) Abou-Sena, et al. [1].

over prediction of gas thermal conductivity. However, such a cut-off mechanism cannot be imposed in the Gusalov's model.

At low gas pressure limit, the effective thermal conductivity predicted by this numerical framework approaches zero. It is because that solid heat conduction contributes little in this point contact mode of the simulated units and helium thermal conductivity approaches zero at low gas pressure as well. Though this can be avoided by introduce a small amount of mechanical loading as shown in Section 3.1, this is not our main focus in the present paper. The prediction made by the Gusalov's model and the SZB model trend towards zero as well since the assumption made in the models is similar to this framework. The Batchelor model gives relative large result at the same low gas pressure limit but a clear decline pointing to zero is reasonable to speculate with gas pressure being lowered further. At high gas pressure limit, the effective thermal conductivity of this work reaches to the saturated conductivity of the SZB model. The Batchelor's model has the highest magnitude and the Gusalov's model is close to it and supposed to exceed the saturated conductivity of the Batchelor's model if gas pressure keeps rising. The Batchelor's model shows over prediction of the effective thermal conductivity, and an offset was suggested to use to fit with experimental data [26].

From comparison, one similarity shared by this framework and the other three models is that the effective thermal conductivity has a positive correlation with the volume fraction and coordination number. It is not surprising that this framework, the Batchelor's model and the Gusalov's model present an upward shift of the effective thermal conductivity against the extent of denseness because the same homogenisation method is employed. Unlike other three models, the SZB model was directly constructed based on volume fraction of beds and accordingly predicts the effective thermal conductivity without the need to assemble contact units. In this case it takes only the volume fraction rather than both of the two characteristics into account, but a shape factor is introduced to compensate lack of consideration about the coordination number. Thus, the denseness has a less significant effect in the SZB model when compared to the other three models.

Even though this framework, the Batchelor's model, and the Gusalov's model using the equal homogenisation equation to predict the effective thermal conductivity of pebble beds based on thermal properties of contact units, the predicted magnitude and behaviour of the effective thermal conductivity of the same pebble bed are different. At contact unit level, the original Batchelor's model neglected the Smoluchowski effect and thus the original model has no gas pressure dependency and size dependency. For a

contact unit of given length and material, the Gusalov's model predicts conductivity increases only depends upon the increase of gas pressure, implying that conductivity increase only when the Knudsen number decreases. Therefore, for a given gas pressure, meaning a given gas mean free path, conductivity increases as the length of contact units increases. However, both of the Bachelor's model and the Gusalov model hold the assumption that thermal conductivity of pebbles is much higher than that of gas, which is the reason why the effective thermal conductivity given by these two models is relatively high. Such an assumption restricts application of these two models. Our model for the contact unit considers the Knudsen number in the gap region, and therefore the gas and size dependency is presented in the model prediction.

3.4. Experimental validation

The effective thermal conductivity of pebble beds measured by hot wire method [1,31] is compared with the result predicted by this work, shown in Fig. 8. The prediction used parameters directly from the experiments, e.g., volume fraction, pebble size distribution, gas pressure and temperature (but the size distribution of Ref. [1] can hardly be found and so the same average size and coordination number were used). The experimental data show that the effective thermal conductivity presents an increasing with the increase of gas pressure within the measurement range. This numerical framework captures this gas pressure dependency shown by the corresponding experimental data. Compared with the corresponding effective thermal conductivity of pebble bed measured by KIT, the predicted result is about 20% lower. The discrepancy between the high temperature result of this work and the corresponding experiments data of Ref. [1] is relatively large and the numerical result is lower as well. However, the numerical result presents a similar gas pressure dependency in the entire gas pressure range. It demonstrates the validity of application of the Smoluchowski effect.

Several reasons may contribute to quantitative discrepancy between this work and the experimental data. First, due to point-contact assumption in establishment of contact units, solid heat conduction at contact points is ignored. However, a contact zone of a finite area always exists in a real contact unit and hence enhances heat transfer ability of a contact unit, increasing the effective thermal conductivity. With elevation of temperature, thermal radiation gains importance. It may be the reason leading the uncertainty. Since coordination number of pebble beds cannot be experimentally detected easily like volume fraction, the coordination number

is estimated based on the volume fraction. So this estimation method may introduce some discrepancy. Furthermore, a refined method to consider size distribution of pebble bed can contribute to more accurate predictions under the proposed numerical framework.

4. Conclusion

A numerical framework consisted of a finite element simulation and a semi-analytical relation is established to predict the effective thermal conductivity of Li_4SiO_4 pebble beds. The predicted result captures gas pressure dependency of the effective thermal conductivity correctly and fits the experimental data of the investigated pebble bed with acceptable discrepancy. Gas pressure effect on thermal transport behaviour of pebble beds is extensively studied and discussed in this work. The effective thermal conductivity of pebble beds is positively correlated to gas pressure and converges at high gas pressure. Such macro-scale phenomenon is resulted from properties of contact units of particle scale. In particle scale, the Smoluchowski effect was taken into account by considering the Knudsen number. As a result, reducing particle size or gas pressure causes decline of the effective thermal conductivity of contact units and hence of pebble beds. The proposed numerical framework is useful to predict the effective thermal conductivity of the pebble beds, and optimise thermal performance of tritium breeding by tuning purge gas pressure and adjusting cooling systems. The framework introduced in this study is ready to extend to investigate other types of granular materials, especially those materials in various applications comprising spherical particles, including thermal insulation, food production and heat exchangers.

Acknowledgement

Financial support for this research from the Australia Research Council through grant DE130101639 is greatly appreciated.

References

- [1] A. Abou-Sena, A. Ying, M. Abdou, Effective thermal conductivity of lithium ceramic pebble beds for fusion blankets: a review, *Fusion Sci. Technol.* 47 (2005) 7.
- [2] D. Aquaro, N. Zaccari, Experimental and numerical analyses on LiSO_4 and Li_2TiO_3 pebble beds used in a ITER test blanket module, *J. Nucl. Mater.* 367–370 (2007) 1293–1297, Part B.
- [3] M. Dalle Donne, A. Goraieb, G. Piazza, G. Sordon, Measurements of the effective thermal conductivity of a Li_4SiO_4 pebble bed, *Fusion Eng. Des.* 49–50 (2000) 513–519.
- [4] F. D'Aleo, P.A. Di Maio, G. Vella, On the Improved current pulse method for the thermal diffusive characterization of lithiated ceramic pebble beds, *Appl. Therm. Eng.* 49 (2012) 48–54.
- [5] A. Abou-Sena, F. Arbeiter, L.V. Boccaccini, G. Schindlwein, Measurements of the purge helium pressure drop across pebble beds packed with lithium orthosilicate and glass pebbles, *Fusion Eng. Des.* 89 (2014) 1459–1463.
- [6] J. Reimann, S. Hermsmeyer, Thermal conductivity of compressed ceramic breeder pebble beds, *Fusion Eng. Des.* 61–62 (2002) 345–351.
- [7] Y. Feng, K. Feng, Y. Liu, B. Gong, Y. Cheng, Experimental investigation of thermal properties of the Li_4SiO_4 pebble beds, *J. Plasma Fusion Res.* 11 (SERIES) (2015).
- [8] Mikio Enoda, Yoshihiro Ohara, Nicole Roux, Alice Ying, Giovanni Pizza, Siegfried Malang, Effective Thermal Conductivity Measurement of the Candidate Ceramic Breeder Pebble Beds by the Hot Wire Method, American Nuclear Society, La Grange Park, IL, 2001, pp. 890, ETATS-UNIS.
- [9] M. Dalle Donne, A. Goraieb, R. Huber, B. Schmitt, G. Schumacher, G. Sordon, A. Weisenburger, Heat transfer and technological investigations on mixed beds of beryllium and Li_4SiO_4 pebbles, *J. Nucl. Mater.* 212 (1994) 872–876.
- [10] A. Abou-Sena, A. Ying, M. Abdou, Experimental measurements of the effective thermal conductivity of a lithium titanate (Li_2TiO_3) pebbles-packed bed, *J. Mater. Process. Technol.* 181 (2007) 206–212.
- [11] M. Panchal, P. Chaudhuri, J.T. Van Lew, A. Ying, Numerical modelling for the effective thermal conductivity of lithium meta titanate pebble bed with different packing structures, *Fusion Eng. Des.* 112 (2016) 303–310.
- [12] Fatollah Tehranian, M.A. Abdou, Experimental study of the effect of external pressure on particle bed effective thermal properties, *Fusion Sci. Technol.* 27 (1995).
- [13] H. Tanigawa, T. Hatano, M. Enoda, M. Akiba, Effective thermal conductivity of a compressed Li_2TiO_3 pebble bed, *Fusion Eng. Des.* 75–79 (2005) 801–805.
- [14] A.V. Gusarov, E.P. Kovalev, Model of thermal conductivity in powder beds, *Phys. Rev. B* 80 (024202) (2009), 024202(024202)024212.
- [15] A.J. Slavin, V. Arcas, C.A. Greenhalgh, E.R. Irvine, D.B. Marshall, Theoretical model for the thermal conductivity of a packed bed of solid spheroids in the presence of a static gas, with no adjustable parameters except at low pressure and temperature, *Int. J. Heat Mass Transfer* 45 (2002) 4151–4161.
- [16] L. Pan, L. Lu, J. Wang, X. Qiu, Modeling the effect of gas on the effective thermal conductivity of heterogeneous materials, *Int. J. Heat Mass Transfer* 90 (2015) 358–363.
- [17] L. Chen, X. Ma, X. Cheng, K. Jiang, K. Huang, S. Liu, Theoretical modeling of the effective thermal conductivity of the binary pebble beds for the CFETR-WCCB blanket, *Fusion Eng. Des.* 101 (2015) 148–153.
- [18] A.V. Gusarov, Transition regime of gas-phase heat transfer in powder beds, *AIP Conf. Proc.* 762 (2005) 294–299.
- [19] H. Petersen, The Properties of Helium: Density, Specific Heats, Viscosity, and Thermal Conductivity at Pressures from 1 to 100 bar and from Room Temperature to About 1800 K, 1970.
- [20] S.S. Kistler, The relation between heat conductivity and structure in silica aerogel, *J. Phys. Chem.* 39 (1934) 79–86.
- [21] ABAQUS Documentation, RI, USA, 2013.
- [22] H.P. Zhu, Z.Y. Zhou, R.Y. Yang, A.B. Yu, Discrete particle simulation of particulate systems: a review of major applications and findings, *Chem. Eng. Sci.* 63 (2008) 5728–5770.
- [23] Y. Gan, Francisco Hernandez, Dorian Hanaor, Ratna Annabattula, Marc Kamlah, Pavel Pereslavtsev, Thermal discrete element analysis of EU solid breeder blanket subjected to neutron irradiation, *Fusion Sci. Technol.* 66 (2014) 83–90.
- [24] Y. Gan, M. Kamlah, J. Reimann, Computer simulation of packing structure in pebble beds, *Fusion Eng. Des.* 85 (2010) 1782–1787.
- [25] G.K. Batchelor, Transport properties of two-phase materials with random structure, *Annu. Rev. Fluid Mech.* 6 (1974) 227–255.
- [26] G.K. Batchelor, R.W. O'Brien, Thermal and electrical conduction through a granular material, *R. Soc. Proc. A* 355 (1977) 313–333.
- [27] T. Aste, M. Saadatfar, T.J. Senden, Local and global relations between the number of contacts and density in monodisperse sphere packs, *J. Stat. Mech.* 2006 (2006) P07010.
- [28] M. Suzuki, T. Oshima, Estimation of the Co-ordination number in a multi-component mixture of spheres, *Powder Technol.* 35 (1983) 159–166.
- [29] M. Suzuki, T. Oshima, Co-ordination number of a multi-component randomly packed bed of spheres with size distribution, *Powder Technol.* 44 (1985) 213–218.
- [30] G.A. Georgalli, M.A. Reuter, Modelling the co-ordination number of a packed bed of spheres with distributed sizes using a CT scanner, *Miner. Eng.* 19 (2006) 246–255.
- [31] S. Pupeschi, R. Knitter, M. Kamlah, Effective thermal conductivity of advanced ceramic breeder pebble beds, *Fusion Eng. Des.* 116 (2017) 73–80.
- [32] M. Abdou, M. Tillack, A. Raffray, A. Hadid, J. Bartlit, C. Bell, P. Gierszewski, J. Gordon, T. Iizuka, C. Kim, Modeling, Analysis and Experiments for Fusion Nuclear Technology: FNT Progress Report: Modeling and FINESSE, California Univ., Los Angeles (USA) Dept. of Mechanical, Aerospace and Nuclear Engineering, 1987.
- [33] M. Akiyama, Design technology of fusion reactors, in: World Scientific, 1991.
- [34] Y. Gan, M. Kamlah, Discrete element modelling of pebble beds: with application to uniaxial compression tests of ceramic breeder pebble beds, *J. Mech. Phys. Solids* 58 (2010) 129–144.